Uptake, translocation, size characterization and localization of cerium oxide nanoparticles in radish (Raphanus sativus L.)

Justyna Wojcieszek, Javier Jiménez-Lamana, Katarzyna Bierla, Lena Ruzik, Monika Asztemborska, Maciej Jarosz, Joanna Szpunar

Uptake, translocation, size characterization and localization of cerium oxide nanoparticles in radish (*Raphanus sativus* L.)

Justyna Wojcieszek[a], Javier Jiménez-Lamana[b,*], Katarzyna Bierła[b], Lena Ruzik[a], Monika Asztemborska[c], Maciej Jarosz[a], Joanna Szpunar[b]

[a] Chair of Analytical Chemistry, Faculty of Chemistry, Warsaw University of Technology, Poland

[b] Institute of Analytical Sciences and Physico-Chemistry for Environment and Materials (IPREM), CNRS-UPPA, UMR5254, Pau, France

[c] Isotopic Laboratory, Faculty of Biology, University of Warsaw, Warsaw, Poland

*Corresponding author: j.jimenez-lamana@univ-pau.fr Telephone: +33540175037

Abstract

Due to their unique physical and chemical properties, the production and use of cerium oxide nanoparticles (CeO_2 NPs) in different areas, especially in automotive industry, is rapidly increasing, causing their presence in the environment. Released CeO_2 NPs can undergo different transformations and interact with the soil and hence with plants, providing a potential pathway for human exposure and leading to serious concerns about their impact on the ecosystem and human organism. This study investigates the uptake, bioaccumulation, possible translocation and localization of CeO_2 NPs in a model plant (*Raphanus sativus* L.), whose edible part is in direct contact with the soil where contamination is more likely to happen. The stability of CeO_2 NPs in plant growth medium as well as after applying a standard enzymatic digestion procedure was tested by single particle ICP-MS (SP-ICP-MS) showing that CeO_2 NPs can remain intact after enzymatic digestion; however, an agglomeration process was observed in the growth medium already after one day of cultivation. An enzymatic digestion method was next used in order to extract intact nanoparticles from the tissues of plants cultivated from the stage of seeds, followed by size characterization by SP-ICP-MS. The results

obtained by SP-ICP-MS showed a narrower size distribution in the case of roots suggesting preferential uptake of smaller nanoparticles which led to the conclusion that plants do not take up the CeO_2 NPs agglomerates present in the medium. However, nanoparticles at higher diameters were observed after analysis of leaves plus stems. Additionally, a small degree of dissolution was observed in the case of roots. Finally, after CeO_2 NPs treatment of adult plants, the spatial distribution of intact CeO_2 NPs in the radish roots was studied by laser ablation ICP-MS (LA-ICP-MS) and the ability of NPs to enter and be accumulated in root tissues was confirmed.

Keywords: Single particle ICP-MS, edible plants, engineered nanoparticles, laser ablation ICP-MS, ionization efficiency

1. Introduction

In recent years there has been a rapid increase in the development, production and application of engineered nanoparticles (ENPs), which are currently playing a growing role in a wide range of industrial and commercial applications (Stark et al., 2015; Vance et al., 2015). Due to their unique properties and novel features, the global production of nanomaterials is significantly increasing, leading to the release of ENPs into the environment, where they can interact with higher plants.

Among the different ENPs, cerium oxide nanoparticles (CeO_2 NPs) are one of the most important and promising due to their capability for undergoing a redox-cycle between the two natural oxidation states (Ce^{3+} and Ce^{4+}) (Cassee et al., 2011), with an estimated global production of up to 10 000 tons per year (Keller et al., 2013; Piccinno et al., 2012). Cerium is the most abundant rare earth element in the earth's crust and belongs to the group of elements referred to as technology-critical elements that were considered just as laboratory curiosities, being now key components for the development of new technologies (Wojcieszek et al., 2018). CeO_2 NPs have special electrical, optical and thermal properties which make them widely used as polishing agents, UV-blockers, glass additives, in agricultural products and especially in automotive industry (Stanek et al., 2008; The Project on EmergingNanotechnologies, 2019; Yang et al., 2017). Moreover, the high reactive oxygen

53 species (ROS) scavenging properties gives CeO_2 NPs the potential to be used as an antioxidant and
54 radioprotective agent (Li et al., 2015). For instance, CeO_2 NPs are widely used in the production of
55 catalysts or as a diesel fuel additive to increase fuel combustion efficiency, decrease diesel soot
56 emissions and to reduce NOx emissions (Cassee et al., 2011; Johnson and Park, 2012). Therefore,
57 their release into the ecosystem is unavoidable for example through deposition along roadways that
58 leads to their translocation to the soil and thus to plants, which has raised serious concerns about their
59 fate and impact in the ecosystem (Colvin, 2003; Gardea-torresdey et al., 2014; Johnson and Park,
60 2012). CeO_2 NPs can interact with the soil and hence with plants, which in turn increase the risk of
61 their bioaccumulation in the animal and human food chain (Colvin, 2003; Deng et al., 2014). As a
62 results, and due to the importance of the physicochemical states of Ce to its food safety implications, a
63 more extensive studies on the interaction of CeO_2 NPs and higher plants is essential for a fully
64 understanding of their environmental impact (W. Zhang et al., 2017a).

65 Both positive and negative effects of CeO_2 NPs on plants have been demonstrated, depending
66 on the plant species, size and concentration of NPs, exposure time and plant growth conditions (Ma et
67 al., 2010; Rossi et al., 2016; Wang et al., 2012; Zhao et al., 2014). Species-dependent responses of
68 plants for CeO_2 NPs treatment have been also observed by other researchers (Lopez-Moreno et al.,
69 2010b). Additionally, it was already presented that toxicity of CeO_2 NPs towards plants is
70 concentration dependent (Lopez-Moreno et al., 2010a). On the other hand, CeO_2 NPs were shown to
71 enhance plant growth under certain exposure conditions (Ma et al., 2016; Wang et al., 2012). CeO_2
72 NPs have generally been considered as insoluble under environmental conditions (Walser et al., 2012)
73 (Yokel et al., 2009). However, several studies suggest that after CeO_2 NPs treatment, cerium in plants
74 could exist in the form of Ce salts or dissolved Ce; reducing agents present in plant growth media
75 could reduce the surface Ce^{4+} of CeO_2 NPs into Ce^{3+} (Dan et al., 2016; Schwabe et al., 2014; Zhang et
76 al., 2012; W. Zhang et al., 2017). Additionally, solubility of CeO_2 NPs is also pH dependent
77 (Hernandez-viezcas et al., 2013). Dissolved form of CeO_2 NPs was found for example in cucumber or
78 soybean plants (Hernandez-Viezcas et al., 2016; Zhang et al., 2012). In contrast, other studies showed
79 that CeO_2 NPs did not undergo any transformation in cucumber, alfalfa, tomato and corn seedling
80 (Lopez-Moreno et al., 2010b). Most of the studies performed showed that CeO_2 NPs can be taken up

by plants, but the majority of NPs appeared to remain in root tissues, raising concerns on their accumulation by root vegetables. However, even though the edible tissues of below-ground vegetables have direct contact with NPs contaminated soils, only little attention has been paid to this group of plants (Zhang et al., 2015).

In this context, radish (*Raphanus sativus* L.), a popular vegetable with high global consumption, was chosen to the study since its edible part is in contact with the soil where contamination, through atmospheric dust deposition, is more likely to happen. Taking into account different, often contradictory, results presented in previous works, the main purpose of this study was to investigate the uptake, translocation, characterization and spatial localization of a commercial suspension of CeO_2 NPs in a model edible plant throughout the whole process by using different mass spectrometry based techniques: the stability of the CeO_2 NP in the hydroponic solution was assessed by single particle ICP-MS (SP-ICP-MS); the bioaccumulation of cerium in plants tissues and the translocation factor from roots to leaves was determined by ICP-MS; the presence of CeO_2 NPs in radish tissues was investigated by SP-ICP-MS and their size distributions obtained; finally, the spatial distribution of cerium in roots was studied by laser ablation ICP-MS (LA-ICP-MS).

2. Material and methods

2.1. Samples and reagents

Seeds of radish (*Raphanus sativus* L.) were purchased from Vilmorin Garden (Komorniki, Poland). Analytical or biological reagent grade chemicals and LC-MS grade solvents were purchased from Sigma-Aldrich (Saint Quentin Fallavier, France) unless stated otherwise. Ultra-pure water (18 MΩ cm) obtained with a MiliQ system (Millipore, Guyancourt, France) was used throughout. Hydrogen peroxide from Fisher Scientific (Hampton, NH) and nitric acid (INSTRA-Analysed) from Baker (Deventer, Netherlands) were used for samples digestion. A standard ionic solution of 1000 mg L^{-1} cerium was purchased from Plasma CAL standards (Teddington, UK). Macerozyme R-10 enzyme (pectinase from *Rhizopus* sp., Sigma Aldrich) was used to digest plant

tissues for CeO_2 NPs extraction. Macerozyme R-10 is a multi-component enzyme mixture containing cellulase (0.1 unit per mg), hemicellulase (0.25 unit per mg) and pectinase (0.5 unit per mg).

Aqueous suspension of CeO_2 NPs (40 wt %) with a nominal size of 30-50 nm was purchased from US Research Nanomaterials, Inc. (Houston, TX). A diluted suspension of CeO_2 NPs was prepared daily in ultrapure water by accurately weighing aliquots of the stock suspension after one minute sonication. After dilution and before each analysis, the suspensions were sonicated for approximately 1 min.

2.2. Instrumentation

Homogenization of the plant tissues was performed by a Vibracell 75115 ultrasonic probe (Bioblock Scientific, Illkirch, France) offering a nominal power of 500 W. Incubation of samples was performed in a Grant OLS-200 water bath (Keison Products, Essex, UK). A Branson B2510 ultrasonic bath (Branson, Danbury, CT) was used for sonication of nanoparticles suspensions and enzymatic extracts before SP-ICP-MS analysis. A Digi-Prep system from SCP Science (Quebec, Canada) was used for acid digestion of plant tissues and extracts for the total cerium determination. A centrifuge 5415R (Eppendorf, Hamburg, Germany) was used for the extraction procedure. pH was adjusted by using a FiveEasy pH meter from Mettler Toledo (Columbus, OH).

The determination of the total concentration of cerium in the plant samples was carried out using an Agilent 7500ce ICP-MS (Agilent, Tokyo, Japan) instrument fitted with Ni cones and a 2.5 mm i.d. injector torch. The position of torch and nebulizer gas flow was adjusted each day of work. The working conditions of ICP MS were optimized daily using a 1 $\mu g\ L^{-1}$ solution of $^{7}Li^{+}$, $^{89}Y^{+}$ and $^{205}Tl^{+}$ in 2% (v/v) HNO_3.

2.3. Single particle ICP-MS method

An Agilent 7900 ICP MS equipped with Single Nanoparticle Application Module was used for the characterization of CeO_2 NPs. The default instrumental and data acquisition parameters are listed in Table 1. During analysis ^{140}Ce with a natural abundance of about 88.5 % was monitored. ^{140}Ce is interference-free in ICP-MS analysis which makes this isotope the best choice for analysis of Ce based nanoparticles. SP-ICP-MS analyses were performed in TRA mode using a dwell time of 100

µs, with a total time of analysis of 60 s. The dwell time is a critical parameter when working in single particle mode and the use of microsecond dwell time can improve particle sizing accuracy and counting (Abad-Álvaro et al., 2016). Gold nanoparticle standard reference material with a nominal diameter of 56 nm (RM 8013) was obtained from NIST (Gaithersburg, USA) and was used for determination of transport efficiency, which was calculated by the particle frequency method described by Pace et al. (2011). The sample flow rate was calculated daily by measuring the mass of water taken up by the peristaltic pump for 2 min (this operation was repeated 3 times). After each sample analysis, the software automatically processed the raw data and generated the particle size, particle concentration, size distribution and information about concentration of dissolved metal. The size distributions were prepared in Origin 8.5 software (Northampton, MA) and adjusted to lognormal distributions in order to obtain the median diameter.

Table 1

Default instrumental and data acquisition parameters for SP-ICP-MS.

Instrumental parameters	
RF Power	1550 W
Argon gas flow rate	
Plasma	15 L min^{-1}
Auxiliary	0.9 L min^{-1}
Nebulizer	1.10 L min^{-1}
Sample uptake rate	0.35 mL min^{-1}
Data acquisition parameters	
Dwell time	100 µs
Readings per replicate	600000
Total acquisition time	60 s
Analyte	Ce
Mass (amu)	140
Density	7.13 g cm^{-3}
Mass fraction	0.8139

2.4. Laser ablation ICP-MS method

A NewWave UP-213 laser ablation (LA) system (NewWave Research, Freemont, USA) was coupled to an Agilent model 7700x (Agilent, Tokyo, Japan) using a 60 cm Tygon tube (5.0 mm i.d.). The laser ablation system was operated in a focused spot mode at the repetition rate of 20 Hz with a spot size of 250 μm and a scan speed of 100 μm s^{-1}. The ablated matter was transported into the ICP with He gas (800 mL min^{-1}) and mixed in a T-connector with carrier gas of ICP MS delivered at 1.1 L min^{-1} aerosol (a Micromist nebulizer and a double pass Scott spray chamber were removed from the configuration). No collision/reaction gas was used during analyses. A 1.5 mm i.d. injector torch and Pt cones were used. Pulse energy was of 30% and fluence was 1.45 J cm^{-2}. The ICP-MS instrument was optimized in wet plasma condition before coupling with laser in order to obtain the maximum Ce signal-to-noise ratio.

2.5. Procedures

2.5.1. Plant cultivation

Portions of radish seeds (ca. 1 g) were germinated in distilled water in darkness for 3 days and then the seedlings were transferred to 350 mL opaque containers with a Knop nutrient solution (pH 6.8) and placed in a growth chamber. After 4 days, the CeO_2 NPs suspension was added to the medium at a cerium concentration of 5 mg L^{-1}. As a control variant, plants were left in the nutrient solution without the addition of cerium. Cultivation was carried out for the next 7 days in a growth chamber. The plants were grown at with a temperature varying from 21-25 °C, light intensity 200 microeinsteins m^{-2} s^{-1}, 12 h photoperiod and 50-60% relative humidity. All the time the solutions in the containers were aerated. Each variant of the cultivation was performed in three replicates. After cultivation, the plants were harvested and the roots were gently rinsed with deionized water. The plants were divided into roots and above ground organs (leaves plus stems) and lyophilized. Dried plant material was ground in a mortar before further analysis.

For LA-ICP-MS analysis, radish plants were initially cultivated in typical garden soil in the greenhouse for 4 weeks to obtain well-formed tubers. Next, adult plants of radish, with the taproot diameter of ca. 1.5 cm were conditioned in deionized water for 24 hours and then transferred to opaque containers with suspensions of CeO_2 NPs (50 mL) at concentrations of 5 mg L^{-1} or 50 mg L^{-1}

for 24 and 48 h. After finishing the cultivation, taproots were gently rinsed with deionized water and prepared for further analysis. Each variant of the cultivation was performed in three replicates.

2.5.2. Determination of total cerium content

Samples of leaves and roots (0.025 g) were digested by adding 2.5 mL HNO_3 (c) in a DigiPrep tube and the following temperature program: 30 min of heating up to 65°C and then keeping temperature at 65°C for 4 h. Afterwards, 1 mL of H_2O_2 (c) was added to the samples and the digestion was continued for the next 4 h using the same program. After digestion, the mixtures were cooling down and diluted with ultrapure water to a final volume of 25 mL. Further dilutions were prepared with 2% HNO_3 (v/v), directly before ICP-MS analysis. Two isotopes of cerium (^{140}Ce, ^{142}Ce) were monitored during analysis. The analytical blanks were analyzed in parallel. Quantification was performed by external calibration; a 5 points calibration curve was prepared for cerium concentration in the investigated range from 0.0 to 5.0 ng mL^{-1}. The content of cerium in each sample was calculated as the mean of results obtained for the monitored isotopes, from three replicates of each sample. In order to verify the accuracy of the method, a recovery study was performed. A known amount of CeO_2 NPs suspension (at the same concentration as used for plant cultivation) was spiked into the controls of roots and leaves plus stems and the acid digestion method described above was applied.

2.5.3. Enzymatic digestion method

After cultivation performed on radish seeds, plant tissues were digested enzymatically as reported in previous works (Jiménez-Lamana et al., 2016; Kińska et al., 2018). Briefly, grounded samples of leaves and roots (0.025 g) were homogenized with 8 mL of 2 mM citrate buffer (pH 4.5; adjusted with citric acid) by using an ultrasonic probe. After the end of homogenization, 2 mL of Macerozyme R-10 solution (0.01 g of enzyme powder for roots and 0.05 g of enzyme powder for leaves plus stems, dissolved in 2 mL of ultrapure water) was added to samples and they were next shaken at 37 °C for 24 hours in a water bath with continuous shaking. After digestion, the samples were settle down for approximately 15 min and the obtained suspensions were filtered with a 0.45 µm syringe filter (Sigma Aldrich). The filtered samples were next analyzed by SP-ICP-MS.

205 *2.5.4. Study of the spatial distribution of CeO_2 NPs in radish roots by LA-ICP-MS*

206 After the end of cultivation performed on adult plants, radish roots were washed with
207 ultrapure water in order to remove nanoparticles adsorbed on the surface. Afterwards, fresh roots
208 samples were cut into 150 μm thick slices using the Leica VT1000 S vibrating blade microtome
209 (Leica Biosystems, Wetzlar, Germany). The radish slices were directly mounted onto glass slides
210 coated with double-sided tape to enhance adhesion and kept in a fridge before further treatment. Four
211 repetitions of each root sample were prepared. The prepared slices were next analyzed by means of
212 LA-ICP-MS. The tissue section was systematically scanned (line by line) by a focused laser beam.
213

214 ## 3. Results and discussion

215 *3.1. Cultivation of radish in the presence of nanoparticles and determination of total content of*
216 *cerium*

217 During cultivation, radish plants appeared tolerant to the applied concentration of CeO_2 NPs
218 since no visible phytotoxic effects were observed. Biomass production and tissues hydration did not
219 differ substantially between the control and the CeO_2 NPs treated plants. Some additional studies on
220 the content of photosynthetic pigments showed that plants were not affected by nanoparticles.

221 The determination of the total cerium content in radish tissues was the first step done after the
222 plant cultivation with the CeO_2 NPs suspension, in order to investigate its distribution among the
223 different tissues. Control and CeO_2 NPs treated samples of leaves (together with stems) and roots of
224 radish were analyzed by standalone ICP-MS after samples mineralization. The quantification limit,
225 calculated as 10 times the standard deviation of the blank (n = 3) divided by the sensitivity, was 0.43
226 ng g^{-1}. The results of cerium content were obtained from three independent experiments and are
227 presented in Table 2.
228

229 **Table 2.**
230 Total cerium content in radish tissues from control and CeO_2 NPs treated plants (mean ± standard
231 deviation).

	Control plant samples /µg g^{-1}	CeO_2 NPs treated samples /µg g^{-1}
Leaves + stems	< LOQ	32.9 ± 0.4
Roots	< LOQ	1948 ± 9

232

233 The obtained results showed that cerium is accumulated in analyzed radish tissues. However,
234 the majority of cerium was found in radish roots and only minor part of cerium was transported to
235 above ground organs, which is in good agreement with many studies as discussed below. The
236 translocation factor (TF), defined as the ratio of cerium content in leaves with respect to roots, was
237 0.017. It has been reported that the translocation from roots to shoots is independent of the cerium
238 content in the roots and of the supplied form of cerium (Yang et al., 2017). Taking into account that
239 roots as edible part of radish are in direct contact with the soil where contamination is more likely to
240 happen, the results of the total content are especially important from the point of view of food safety.
241 To determine the accuracy of the proposed acid digestion method, a recovery study was made.
242 Control plant samples (leaves plus stems, and roots) were spiked with a known amount of CeO_2 NPs
243 and the acid digestion method was applied. Good recovery values were obtained for both leaves plus
244 stems (103.2%) and roots (102.7%). Regardless of the total content of cerium determined in plant
245 tissues in previous works, its translocation from roots to the aerial part was always in very low level.
246 For instance, Yang et al. (2017) reported that the TF of cerium from roots to above ground organs in
247 *Arabidopsis thaliana* plant is 0.042, while Rossi et al. (2016) found a TF of around 0.002 after
248 analysis of *Brassica napus* L. In the case of desert plant mesquite, the TF of cerium was 0.2 and 0.25
249 for plants treated with 500 and 4000 mg L^{-1}, respectively (Hernandez-Viezcas et al., 2016). In the case
250 of plants grown in soils, a TF of 0.02–0.03 was found in kidney bean plants (Majumdar et al., 2016).
251 It should be also mentioned that no translocation of cerium to above ground organs was observed in
252 the case of tomato or wheat plants (Antisari et al., 2015; Schwabe et al., 2015). The TF is dependent
253 also on the size of CeO_2 NPs. It was showed that after analysis of pumpkin leaves and roots, the TF
254 for CeO_2 NPs of 9 nm was 0.0004 whereas no cerium translocation was observed in the case of NPs of
255 64 nm (Schwabe et al., 2015).

256 *3.2. Study of ionization efficiency of CeO_2 NPs in the plasma*

The calculations behind SP-ICP-MS theory lie on some assumptions, being a plasma ionization efficiency for nanoparticles comparable to the corresponding dissolved species one of them (Pace et al., 2011). However, while this has proven to be true for silver or gold nanoparticles (Hu et al., 2009; Laborda et al., 2011), it might not be the case for nanoparticles of a different nature, like it has been reported for selenium nanoparticles (Jiménez-Lamana et al., 2018), and needs to be first investigated. A ionization efficiency lower than 100% was reported for CeO_2 NPs with sizes from 1 to 10 nm (Sánchez-garcía et al., 2016). However, this value might be different in the case of the CeO_2 NPs used in this study, since the ablation and ionization may strongly vary while increasing the size of the nanoparticle. In order to calculate the ionization efficiency, the response of the ICP-MS towards the nanoparticulated form of cerium was studied, by determining and comparing the total cerium concentration of digested nanoparticles and a suspension of undigested nanoparticles. The calibration was achieved with aqueous standards of cerium in 2% HNO_3 for the digested nanoparticles and in ultrapure water and in 2% HNO_3 for the direct analysis of the suspension, in order to investigate the influence of the medium on the cerium sensitivity. The concentrations determined in ultrapure water and in 2% HNO_3 for the undigested CeO_2 NPs suspension were 9.7 ± 0.9% and 10.2 ± 1.2% with regard to the concentration determined after acid digestion, respectively (Table 3).

Table 3.

Determination of cerium concentration in digested and undigested suspension of CeO_2 NPs (mean ± standard deviation).

Sample	Total Cerium content / mg L^{-1}
Acid digestion	237.9 ± 3.0
Suspension in ultrapure water	23.1 ± 2.1
Suspension in 2 % HNO_3 (v/v)	24.4 ± 2.9

These results show that ICP-MS sensitivity depends on the physicochemical form of cerium and thus a particle ionization efficiency, defined as the ratio of the ionization efficiency of the particle to the ionization efficiency of the corresponding dissolved metal solution (Pace et al., 2011), needs to be taken into account. According to the results obtained in this study, a particle ionization efficiency

of 10% was applied for sizing CeO_2 NPs. In addition, it was shown that the medium has no significant influence on the ionization of CeO_2 NPs.

The suspension of CeO_2 NPs used in this study was then analysed by means of SP-ICP-MS at a concentration of around $1x10^8$ NP L^{-1} taking into account the ionization efficiency calculated. The size distribution obtained (Fig. 1) showed a polydisperse distribution with its central part within the size range provided by the manufacturer: 30-50 nm.

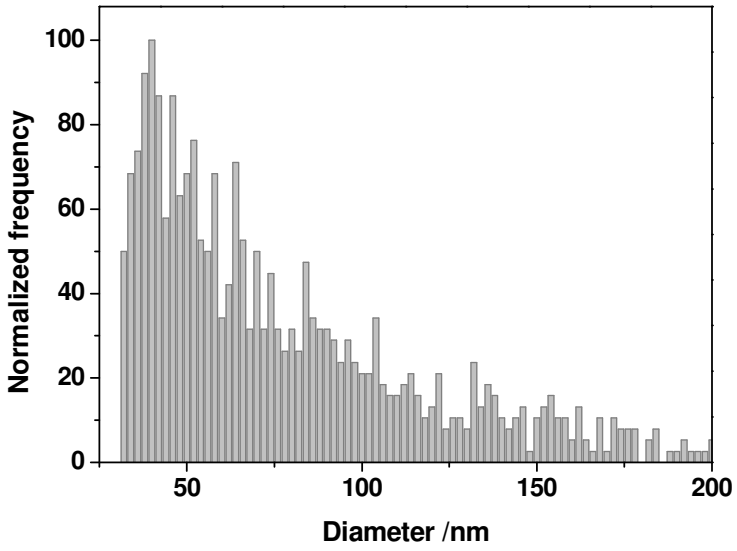

Fig. 1. Size distribution of the commercial suspension of CeO_2 NPs used in the cultivation studies.

3.3 Investigation of CeO_2 NPs stability

3.3.1 Stability in growth medium

Before the analysis of plant samples, the stability of the suspension of CeO_2 NPs in the growth medium was investigated. A suspension of CeO_2 NPs of 5 mg L^{-1} was spiked into the nutrient solution and the size distribution of the nanoparticles was determined by SP-ICP-MS immediately upon preparation and after 1, 2, 4 and 7 days. Each suspension analysed was diluted accordingly in order to measure the same number of events. The median diameters obtained from the corresponding size distributions of nanoparticles at the different times analysed are shown in Table 4. From the results obtained, it can be concluded that CeO_2 NPs undergo agglomeration after 1 day of cultivation in growth medium, with an increase of the median diameter from 56.0 nm to 128.3 nm, whereas the

size distribution does not vary significantly from 1 to 7 days of cultivation (Fig. S1). The agglomeration of CeO_2 NPs has already been observed in hydroponic solution, without the addition of a stabilizing agent (Schwabe et al., 2013; Schwabe et al., 2014). Remarkably, no background signal corresponding to dissolved cerium was observed on the SP-ICP-MS time scans at any of the incubation times tested in the present study. This finding can be explained by two facts: on one hand, the occurrence of CeO_2 NPs agglomerates prevent from cerium dissolution, since agglomeration reduces the effective specific surface area of nanoparticles, which results in less cerium dissolution; on the other hand, the release of cerium ions is size dependent: in a study performed with CeO_2 NPs in Hoagland medium, Schwabe et al. (2014) showed that the smallest particles (9 nm) released the highest amount of cerium, whereas the release of cerium by the largest particles (64 nm) was almost negligible.

Table 4.

Median diameters of CeO_2 NPs suspended in nutrient solution after different contact times.

Incubation time	Median diameter / nm
0	56.0 ± 1.9
1 day	128.3 ± 19.1
2 days	119.1 ± 4.6
4 days	112.5 ± 3.9
7 days	134.6 ± 22.7

3.3.2. Influence of enzymatic digestion and plant matrix

The influence of the enzymatic procedure on the size distribution of the CeO_2 NPs suspension was also studied. For this purpose, a suspension of CeO_2 NPs (5 mg L^{-1}) with no plant tissue was treated with the same conditions of enzymatic digestion. As it can be shown in Fig. 2, the size distribution obtained for enzyme-treated CeO_2 NPs was in good agreement with the size distribution obtained for CeO_2 NPs stock suspension freshly prepared and hence the integrity of CeO_2 NPs is not affected by the enzyme used in the digestion procedure.

In addition, the influence of the plant matrix was investigated. Control leaves plus stems and control roots of radish were spiked with 5 mg L^{-1} of the CeO_2 NPs suspension, submitted to the

enzymatic digestion procedure and the corresponding nanoparticle size distributions obtained by SP-ICP-MS. The size distributions obtained for both spiked tissues were in good agreement with those obtained for freshly enzyme-treated CeO_2 NPs (Fig. 2). These results showed that the procedure proposed can be used to extract CeO_2 NPs from plant tissues without causing their transformation.

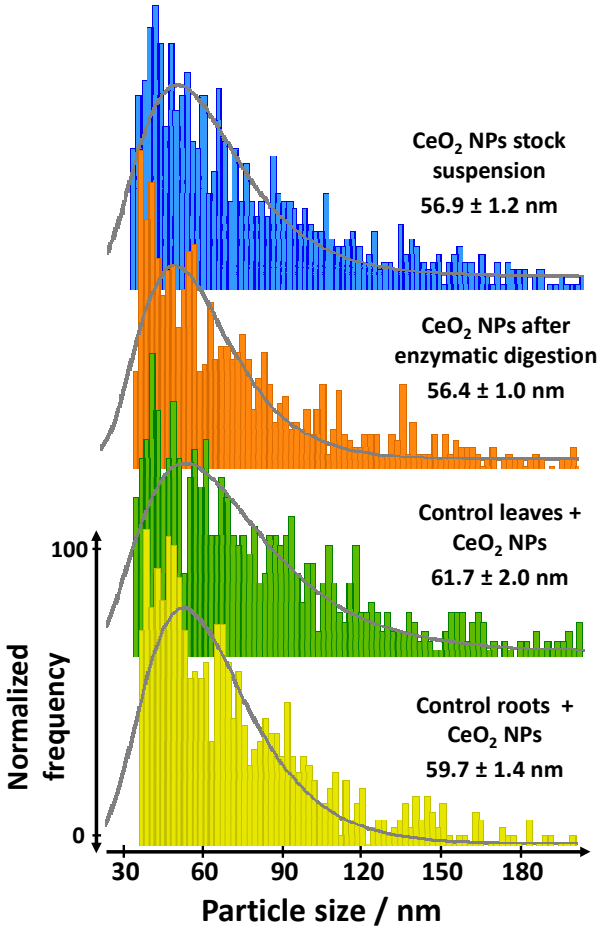

Fig. 2. Size distributions of: CeO_2 NPs stock suspension freshly prepared (blue); CeO_2 NPs after enzymatic digestion procedure (orange); control leaves plus stems (green) and roots (yellow) spiked with 5 mg L^{-1} CeO_2 NPs suspension. Size distributions were adjusted to lognormal distributions (grey line) and the median diameter ± the standard deviation obtained.

3.4. Single particle ICP-MS analysis of leaves plus stems and roots of radish

In order to identify the form of cerium inside the radish tissues cultivated from the stage of seeds, samples of leaves plus stems and samples of roots were subjected to the enzymatic procedure followed by SP-ICP-MS analysis. In a first step, roots and leaves plus stems of control plants were

analyzed and the corresponding time scans obtained (Fig. 3a and 3b, respectively). As expected, only a few pulses above the background were observed for control plants. The presence of these pulses may be explained by a slight contamination of the sonication probe during the enzymatic digestion procedure, but their occurrence is not significant (less than 10 pulses out of 600,000 readings) and hence does not hamper the further analyses.

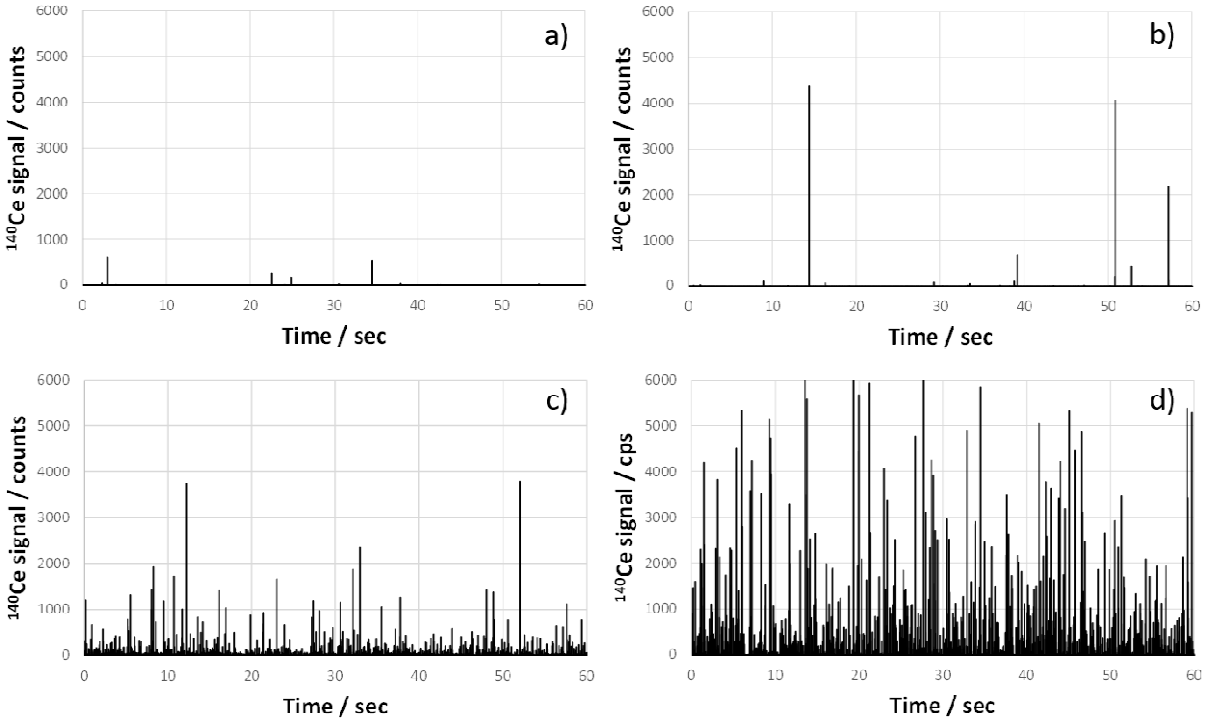

Fig. 3. Time scans obtained for samples of: a) roots, and b) leaves of control plants and for c) roots and d) leaves of plants treated with 5 mg L^{-1} of CeO_2 NPs.

Afterwards, the SP-ICP-MS analyses of CeO_2 NPs treated samples were performed. Samples of roots were diluted 3000 times before analysis whereas samples of leaves plus stems were diluted 200 times. Each tissue was analyzed by triplicate. Time scans obtained showed a significant number of pulses in both plants tissues (Fig. 3c and 3d), proving that radish is able to uptake CeO_2 NPs and transports them into the aerial part of the plant. The presence of CeO_2 NPs has been already reported in tomato (*S. lycopersicum L.*), cucumber (*C. sativus*), pumpkin (*Cucurbita pepo*), and soybean (*Glycine max*) shoots (Dan et al., 2016; Zhang et al., 2011; Zhang et al., 2017b), in *Arabidopsis thaliana* shoots (Yang et al., 2017) and in romain lettuce shoots (P. Zhang et al., 2017a). According to

358 the number of pulses detected, the nanoparticle number concentration in roots and in leaves plus
359 stems was calculated as 3.3 x 10^{11} and 2.4 x 10^{10} NP L^{-1}, respectively. The largest number of number
360 concentration of nanoparticles observed in roots could be explained by a direct contact of roots with
361 CeO_2 NPs suspension. Remarkably, the intensity of the pulses observed in the time scan obtained for
362 leaves is significantly higher than for roots, which suggested the presence of bigger nanoparticles. In
363 addition, no signal corresponding to dissolved cerium was observed for leaves, suggesting that CeO_2
364 NPs did not underwent dissolution during their transport, although small signal coming from
365 dissolved form of cerium was observed for roots. This is in good agreement with other studies that
366 have shown that the dissolution of CeO_2 NPs occur at the root surface rather than inside plants (P.
367 Zhang et al., 2017b). For instance, Ma et al. (2015) shown that dissolution of CeO_2 NPs only occurred
368 at root surfaces, whereas Ce (IV) was not reduced in the tissues in hydroponic cucumber plants. Other
369 authors have reported that plants roots activity have an impact on the dissolution of CeO_2 in
370 hydroponically grown wheat, pumpkin, and sunflower plants (Schwabe et al., 2015).

371 Due to the small signal coming from dissolved form of cerium observed after analysis of roots
372 by SP-ICP-MS, a speciation study was performed by means of size exclusion chromatography (SEC)
373 coupled to ICP-MS. The chromatogram obtained (Fig. S1) showed just one signal coming from high
374 molecular weight cerium compounds which could be explained by the ability of metal ions to create
375 agglomerates even with low molecular weight ligands. However, the extraction efficiency of cerium
376 from radish roots (procedure explained in Supplementary Information), was determined at only 0.19%
377 and therefore, due to negligible presence of cerium compounds, the speciation study of cerium was
378 not continued.

379 From time scans and by applying the ionization efficiency factor calculated before, the size
380 distributions of CeO_2 NPs in radish tissues were obtained. As it can be observed, the particle size
381 distribution obtained for radish roots was narrower (Fig. 4a), with a median diameter of 42.7 nm,
382 suggesting a preferential uptake of NPs at smaller sizes and that the agglomerates present in growth
383 medium already after one day are not taken up by the plant. The finding that plant uptake of CeO_2
384 NPs depends on the particle size and smaller particles are more readily taken up by plants has been
385 previously suggested (Zhang et al., 2011). However, the particle size distribution obtained for leaves

386 plus stems (Fig. 4b), showed a significant number of nanoparticles at higher diameters than in the case
387 of roots (median diameter: 60.3 nm). Since it was found that plants are not able to take up big
388 nanoparticles this finding may be explained by an agglomeration process that takes place at the
389 endpoint of transport of CeO_2 NPs from roots to above ground organs. Once CeO_2 NPs have entered
390 the plant, they are translocated up to above-ground organs through the xylem system, driven by the
391 transpiration stream (Zhao et al., 2013). The endpoint of this transport pathway is the leaves (Zhao et
392 al., 2013), where nutrients and water arrive through the veins. At this point, nanoparticles will be
393 locally more concentrated and hence agglomeration by contact is more likely to occur. Similarly,
394 particle aggregates have been found in leaves of *Arabidopsis thaliana* treated with CeO_2 NPs (Yang et
395 al., 2017).
396
397

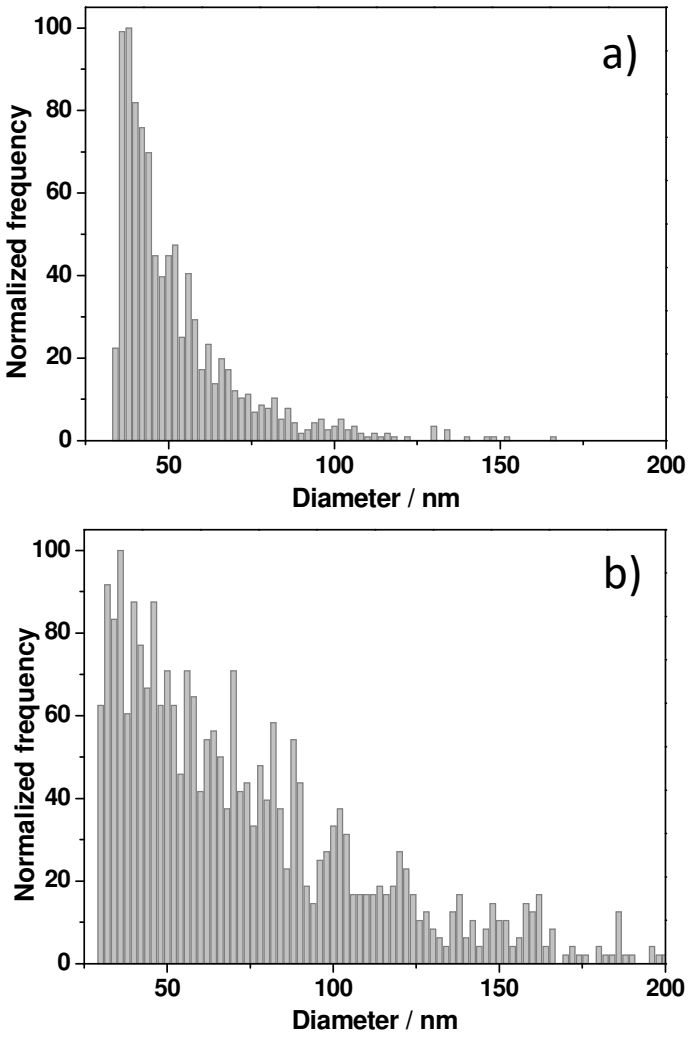

Fig. 4. Size distributions obtained for a) roots, and b) leaves plus stems of radish

The biotransformation of CeO_2 NPs inside plants remains a controversial issue. Some authors have suggested the uptake of Ce(III) followed by re-precipitation as pathway in CeO_2 NPs uptake by plants (Schwabe et al., 2015). However, our study showed that the dissolution of cerium is not significant and thus this mechanism can be discarded. On the other hand, cerium has been shown to be present in the shoots of cucumber and lettuce plants as CeO_2 and cerium carboxylates (Zhang et al., 2012; Zhang et al., 2017a), although the majority of studies have shown that cerium mostly remained as CeO_2 NP in plants tissues (Majumdar et al., 2014; Zhang et al., 2017b). For instance, in a study conducted with romaine lettuce, the amount of cerium carboxylates in leaves was reported at 3.5% (P. Zhang et al., 2017a). These previous findings make us state that the cerium signal observed in radish leaves plus stems is due to CeO_2 NPs and/or aggregates.

3.5. Study of spatial distribution of CeO_2 NPs in radish roots by LA-ICP-MS

The results obtained by SP-ICP-MS analysis showed that the great majority of CeO_2 NPs remain in the form of nanoparticles both in roots and leaves. Therefore, in order to check if CeO_2 NPs have the ability to enter and be accumulated inside the radish tissues, the localization of CeO_2 NPs in the radish roots, as edible part of the plant, was determined by LA-ICP-MS. Analyses were performed after cultivation of radish carried out on adult plants. It is worth to mention that radish belongs to the group of plants with root system in type of taproot, with one central and dominant root. Additionally, taproot of radish is in the shape of fusiform root – The primary root of the system is the widest in the middle with secondary root tapers towards the bottom. Optimisation of a LA-ICP-MS analysis in terms of sensitivity and S/N ratio allowed to choose optimum scan speed of 100 µm s^{-1} and spot size of 250 µm; increase in the laser beam spot size resulted in a considerable gain in sensitivity and homogeneity of the signal as more material is introduced into the plasma per time unit. After analysis of control plants cultivated for 2 days, no signal corresponding to cerium was observed (Fig. 5). The results obtained for radish samples treated with 5 mg L^{-1} of CeO_2 NPs (Fig. 5A) showed peaks from cerium only at the external part of the analysed slices. Nanoparticles were found at a depth of about

1.2 mm leading to the conclusion that CeO_2 NPs have the ability to enter and be accumulated into the radish tissues, which is in good agreement with another study performed with radish in soil (W. Zhang et al., 2017b). Similar situation was observed in the case of radish samples treated with 50 mg L^{-1} CeO_2 NPs (Fig. 5B). Signals from cerium were registered just below the skin surface, with higher intensity than those observed for samples treated with 5 mg L^{-1} CeO_2 NPs. However, one additional signal was observed in the central part of samples after 1 day and 2 days of treatment, which suggest that cerium is accumulated and transported by secondary roots from bottom towards the central part of radish roots, not only through the surface. Accumulation of the metals in the taproot of plants was already observed after a LA-ICP-MS analysis of another root vegetables such as carrot (Yudasari et al., 2018). In addition, two additional signals were observed for samples treated with CeO_2 NPs for two days, suggesting that after accumulation, nanoparticles can be translocated within analysed radish tissues. Moreover, it was observed that the intensity of cerium signals increased with time for both treatments, showing that a higher content of cerium can be accumulated in radish roots with a longer exposure time; a relevant information in terms of food safety taking into account the persistence of CeO_2 NPs in the environment. A good reproducibility of the cerium spatial distribution was achieved after comparing results of the different slices of the same radish root or from different radish roots with the same exposure concentration and time.

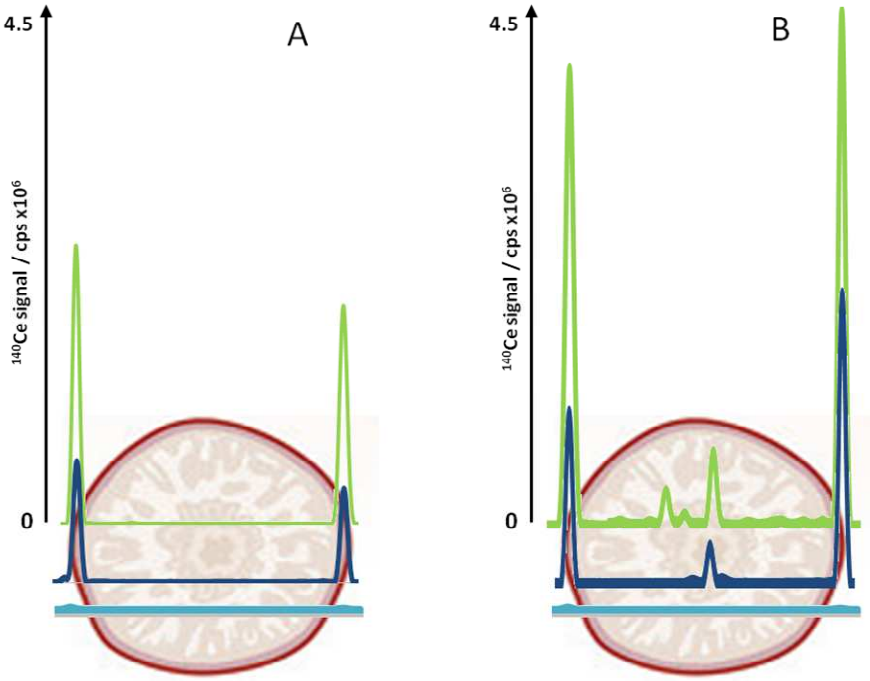

Fig. 5. LA-ICP-MS analysis of radish roots treated with A) 5 mg L^{-1} CeO_2 NPs B) 50 mg L^{-1} CeO_2 NPs. Light blue line: control plant; dark blue line: plants treated for 1 day; green line: plants treated for 2 days

4. Conclusions

The uptake, bioaccumulation, translocation, physico-chemical characterization and localization of CeO_2 NPs in radish was investigated by using different mass spectrometry based techniques. Our results showed that after cultivation, the majority of cerium remain in roots, with a low transportation up to leaves and stems (TF 0.017) as it has been observed in other studies. In order to get a correct particle size distribution, the behavior of CeO_2 NPs in plasma was investigated, showing that ICP-MS sensitivity depends on the physicochemical form of cerium and thus the ionization efficiency must be taken into account. Although CeO_2 NPs underwent agglomeration in hydroponic medium after 1 day, the SP-ICP-MS analysis indicated that radish only takes up small nanoparticles, since the presence of bigger nanoparticles and/or aggregates was not observed. The studies performed discarded interaction with plant matrix or effect of the enzymatic digestion procedure that affected the size of the nanoparticles. However, the analysis of leaves plus stems showed the presence of nanoparticles with bigger sizes, which suggests that nanoparticles undergo agglomeration at the endpoint of their transportation. Finally, the analysis by LA-ICP-MS in radish roots showed that the accumulation of CeO_2 NPs occurs mainly below the skin surface but after accumulation they have the ability to enter and be translocated within the tissue. The results obtained in this work can be consider meaningful from the point of view of food safety.

Acknowledgements

This work was financially supported by the National Science Centre, Poland (grant n° 2015/18/M/ST4/00257) as well as by a STSM Mobility Grant (JW) COST Action TD1407 (grant n° 42007) and the project AQUITRACES Region Aquitaine 20131206001-13010973. Authors would

like to thank Wojciech Kurek (Department of Botany, Warsaw University of Life Sciences (SGGW)) for preparation of samples for LA-ICP-MS analysis.

Appendix A. Supplementary data

Electronic supplementary information (ESI) available: procedure of extraction and fractionation of Ce species from radish samples by SEC-ICP-MS; size distributions of CeO_2 NPs in grow medium at different incubation times; SEC-ICP-MS chromatogram of ammonium acetate extract of radish roots.

References

Abad-Álvaro, I., Peña-Vázquez, E., Bolea, E., Bermejo-Barrera, P., Castillo, J.R., Laborda, F., 2016. Evaluation of number concentration quantification by single-particle inductively coupled plasma mass spectrometry: microsecond vs. millisecond dwell times. Anal. Bioanal. Chem. 408, 5089–5097. https://doi.org/10.1007/s00216-016-9515-y

Antisari, L.V., Carbone, S., Gatti, A., Vianello, G., Nannipieri, P., 2015. Uptake and translocation of metals and nutrients in tomato grown in soil polluted with metal oxide (CeO 2 , Fe 3 O 4 , SnO 2 , TiO 2) or metallic (Ag , Co , Ni) engineered nanoparticles. Env. Sci Pollut Res 1841–1853. https://doi.org/10.1007/s11356-014-3509-0

Cassee, F.R., Balen, E.C. Van, Singh, C., Green, D., Muijser, H., 2011. Exposure , health and ecological effects review of engineered nanoscale cerium and cerium oxide associated with its use as a fuel additive. Crit. Rev. Toxicol. 41, 213–229. https://doi.org/10.3109/10408444.2010.529105

Colvin, V.L., 2003. The potential environmental impact of engineered nanomaterials. Nat. Biotechnol. 21, 1166–1170.

Dan, Y., Ma, X., Zhang, W., Liu, K., 2016. Single particle ICP-MS method development for the determination of plant uptake and accumulation of CeO 2 nanoparticles. Anal. Bioanal. Chem. 408, 5157–5167. https://doi.org/10.1007/s00216-016-9565-1

Deng, Y., White, J.C., Xing, B., 2014. Interactions between engineered nanomaterials and agricultural crops : implications for food safety *. J. Zhejiang Univ. Sci. A：Applied Phys. Eng. 15, 552–572. https://doi.org/10.1631/jzus.A1400165

Gardea-torresdey, J.L., Rico, C.M., White, J.C., 2014. Trophic Transfer, Transformation, and Impact of Engineered Nanomaterials in Terrestrial Environments. Environ. Sci. Technol. 48, 2529–2540. https://doi.org/10.1021/es4050665

Hernandez-viezcas, J.A., Castillo-michel, H., Andrews, J.C., Cotte, M., Rico, C., Peralta-videa, J.R.,

Ge, Y., Priester, J.H., Holden, A., Gardea-torresdey, J.L., 2013. In Situ Synchrotron X - ray Fluorescence Mapping and Speciation of CeO 2 and ZnO Nanoparticles in Soil Cultivated Soybean (Glycine max). ACS Nano 7, 1415–1423. https://doi.org/10.1021/nn305196q

Hernandez-Viezcas, J.A., Castillo-michel, H., Peralta-Videa, J.R., Gardea-Torresdey, J.L., 2016. Interactions between CeO 2 Nanoparticles and the Desert Plant Mesquite: A Spectroscopy Approach. ACS Sustain. Chem. Eng. 4, 1187–1192. https://doi.org/10.1021/acssuschemeng.5b01251

Hu, S., Liu, R., Zhang, S., Huang, Z., Xing, Z., Zhang, X., 2009. A New Strategy for Highly Sensitive Immunoassay Based on Single-Particle Mode Detection by Inductively Coupled Plasma. https://doi.org/10.1016/j.jasms.2009.02.005

Jiménez-Lamana, J., Abad-Álvaro, I., Katarzyna, B., Laborda, F., Szpunar, J., Lobinski, R., 2018. Detection and characterization of biogenic selenium nanoparticles in selenium-rich yeast by single particle ICPMS. J. Anal. At. Spectrom. 33, 452–460. https://doi.org/10.1039/C7JA00378A

Jiménez-Lamana, J., Wojcieszek, J., Jakubiak, M., Asztemborska, M., Szpunar, J., 2016. Single particle ICP-MS characterization of platinum nanoparticles uptake and bioaccumulation by Lepidium sativum and Sinapis alba plants. J. Anal. At. Spectrom. 31, 2321–2329. https://doi.org/10.1039/C6JA00201C

Johnson, A.C., Park, B., 2012. Predicting contamination by the fuel additive cerium oxide engineered nanoparticles within the United Kingdom and the associated risks. Environ. Toxicol. Chem. 31, 2582–2587. https://doi.org/10.1002/etc.1983

Keller, A.A., Mcferran, S., Lazareva, A., Suh, S., 2013. Global life cycle releases of engineered nanomaterials. J Nanopart Res 15, 1692. https://doi.org/10.1007/s11051-013-1692-4

Kińska, K., Jiménez-Lamana, J., Kowalska, J., Krasnodębska-Ostręga, B., Szpunar, J., 2018. Study of the uptake and bioaccumulation of palladium nanoparticles by Sinapis alba using single particle ICP-MS. Sci. Total Environ. 615, 1078–1085. https://doi.org/10.1016/j.scitotenv.2017.09.203

Laborda, F., Jiménez-Lamana, J., Bolea, E., Castillo, J.R., 2011. Selective identification, characterization and determination of dissolved silver(i) and silver nanoparticles based on single particle detection by inductively coupled plasma mass spectrometry. J. Anal. At. Spectrom. 26, 1362. https://doi.org/10.1039/c0ja00098a

Li, Y., He, X., Yin, J., Ma, Y., Zhang, P., Li, J., Ding, Y., 2015. Acquired Superoxide-Scavenging Ability of Ceria Nanoparticles **. Angew. Chemie - Int. Ed. 54, 1832–1835. https://doi.org/10.1002/anie.201410398

Lopez-Moreno, M.L., De la Rosa, G., Hernandez-Viezcas, J.A., Castillo-michel, H., Botez, C.E., Peralta-Videa, J.R., Gardea-Torresdey, J.L., 2010a. Evidence of the Differential Biotransformation and Genotoxicity of ZnO and CeO 2 Nanoparticles on Soybean (Glycine max) Plants. Environ. Sci. Technol. 44, 7315–7320.

539 Lopez-Moreno, M.L., De la Rosa, G., Hernandez-Viezcas, J.A., Peralta-Videa, J.R., Gardea-
540 Torresday, J.L., 2010b. X-ray Absorption Spectroscopy (XAS) Corroboration of the Uptake
541 and Storage of CeO 2 Nanoparticles and Assessment of Their Differential Toxicity in Four
542 Edible Plant Species. J. Agric. Food Chem. 58, 3689–3693. https://doi.org/10.1021/jf904472e
543 Ma, X., Geiser-lee, J., Deng, Y., Kolmakov, A., 2010. Interactions between engineered nanoparticles (
544 ENPs) and plants : Phytotoxicity , uptake and accumulation. Sci. Total Environ. 408, 3053–
545 3061. https://doi.org/10.1016/j.scitotenv.2010.03.031
546 Ma, X., Wang, Q., Rossi, L., Ebbs, S.D., White, J.C., 2016. Multigenerational exposure to cerium
547 oxide nanoparticles : Physiological and biochemical analysis reveals transmissible changes in
548 rapid cycling Brassica rapa. NanoImpact 1, 46–54. https://doi.org/10.1016/j.impact.2016.04.001
549 Ma, Y., Zhang, P., Zhang, Z., He, X., Zhang, Junzhe, Ding, Y., Zhang, Jing, Zheng, L., Guo, Z.,
550 Zhang, L., Chai, Z., Zhao, Y., 2015. Where Does the Transformation of Precipitated Ceria
551 Nanoparticles in Hydroponic Plants Take Place? Environ. Sci. Technol. 9, 10667−10674.
552 https://doi.org/10.1021/acs.est.5b02761
553 Majumdar, S., Peralta-videa, J.R., Bandyopadhyay, S., 2014. Exposure of cerium oxide nanoparticles
554 to kidney bean shows disturbance in the plant defense mechanisms. J. Hazard. Mater. 278, 279–
555 287. https://doi.org/10.1016/j.jhazmat.2014.06.009
556 Majumdar, S., Peralta-videa, J.R., Trujillo-reyes, J., Sun, Y., Barrios, A.C., Niu, G., Margez, J.P.F.-,
557 Gardea-torresdey, J.L., 2016. Science of the Total Environment Soil organic matter in fl uences
558 cerium translocation and physiological processes in kidney bean plants exposed to cerium oxide
559 nanoparticles. Sci. Total Environ. 569–570, 201–211.
560 https://doi.org/10.1016/j.scitotenv.2016.06.087
561 Pace, H.E., Rogers, N.J., Jarolimek, C., Coleman, V.A., Higgins, C.P., Ranville, J.F., 2011.
562 Determining Transport Efficiency for the Purpose of Counting and Sizing Nanoparticles via
563 Single Particle Inductively Coupled Plasma Mass Spectrometry. Anal. Chem. 83, 9361–9369.
564 https://doi.org/10.1021/ac201952t
565 Piccinno, F., Gottschalk, F., Seeger, S., Nowack, B., 2012. Industrial production quantities and uses of
566 ten engineered nanomaterials in Europe and the world. J Nanopart Res 14, 1109.
567 https://doi.org/10.1007/s11051-012-1109-9
568 Rossi, L., Zhang, W., Lombardini, L., Ma, X., 2016. The impact of cerium oxide nanoparticles on the
569 salt stress responses of Brassica napus L . *. Environ. Pollut. 219, 28–36.
570 https://doi.org/10.1016/j.envpol.2016.09.060
571 Sánchez-garcía, L., Bolea, E., Laborda, F., Cubel, C., Ferrer, P., Gianolio, D., Silva, I., Castillo, J.R.,
572 2016. Size determination and quantification of engineered cerium oxide nanoparticles by flow
573 field-flow fractionation coupled to inductively coupled plasma mass spectrometry. J.
574 Chromatogr. A 1438, 205–215. https://doi.org/10.1016/j.chroma.2016.02.036
575 Schwabe, F., Schulin, R., Limbach, L.K., Stark, W., Bürge, D., Nowack, B., 2013. Influence of two

types of organic matter on interaction of CeO 2 nanoparticles with plants in hydroponic culture. Chemosphere 91, 512–520. https://doi.org/10.1016/j.chemosphere.2012.12.025

Schwabe, F., Schulin, R., Rupper, P., Rotzetter, A., Stark, W., Nowack, B., 2014. Dissolution and transformation of cerium oxide nanoparticles in plant growth media. J. Nanoparticle Res. 16, 2668. https://doi.org/10.1007/s11051-014-2668-8

Schwabe, F., Tanner, S., Schulin, R., Rotzetter, A., Stark, W., Quadt, A. Von, Nowack, B., 2015. Dissolved cerium contributes to uptake of Ce in the three crop plants †. Metallomics 7, 466–477. https://doi.org/10.1039/C4MT00343H

Stanek, C.R., Tan, A.H.H., Owens, S.L., Grimes, Æ.R.W., 2008. Atomistic simulation of CeO 2 surface hydroxylation : implications for glass polishing. J Mater Sci 43, 4157–4162. https://doi.org/10.1007/s10853-008-2605-2

Stark, W.J., Stoessel, P.R., Wohlleben, W., Hafner, A., 2015. Industrial applications of nanoparticles. Chem Soc Rev 44, 5793–5805. https://doi.org/10.1039/c4cs00362d

Vance, M.E., Kuiken, T., Vejerano, E.P., McGinnis, S.P., Hochella, M.F., Hull, D.R., 2015. Nanotechnology in the real world: Redeveloping the nanomaterial consumer products inventory. Beilstein J. Nanotechnol. 6, 1769–1780. https://doi.org/10.3762/bjnano.6.181

Walser, T., Limbach, L.K., Brogioli, R., Erismann, E., Flamigni, L., Hattendorf, B., Juchli, M., Krumeich, F., Ludwig, C., Prikopsky, K., Rossier, M., Saner, D., Sigg, A., Hellweg, S., Gu, D., Stark, W.J., 2012. Persistence of engineered nanoparticles in a municipal solid-waste incineration plant. Nat. Nanotechnol. 7, 6–11. https://doi.org/10.1038/NNANO.2012.64

Wang, Q., Ma, X., Zhang, W., Peia, H., Chen, Y., 2012. The impact of cerium oxide nanoparticles on tomato (Solanum lycopersicum L .) and its implications for food safety. Metallomics 4, 1105–1112. https://doi.org/10.1039/c2mt20149f

Wojcieszek, J., Szpunar, J., Lobinski, R., 2018. Speciation of technologically critical elements in the environment using chromatography with element and molecule specific detection. Trends Anal. Chem. 104, 42–53. https://doi.org/10.1016/j.trac.2017.09.018

Yang, X., Pan, H., Wang, P., Zhao, F., 2017. Particle-specific toxicity and bioavailability of cerium oxide (CeO 2) nanoparticles to Arabidopsis thaliana. J. Hazard. Mater. 322, 292–300. https://doi.org/10.1016/j.jhazmat.2016.03.054

Yokel, R.A., Florence, R.L., Unrine, J.M., Tseng, M.T., Graham, U.M., Wu, P., Grulke, E.A., Sultana, R., Hardas, S.S., Butterfield, D.A., 2009. Biodistribution and oxidative stress effects of a systemically-introduced commercial ceria engineered nanomaterial. Nanotechnology 3, 234–249. https://doi.org/10.1080/17435390902974496

Yudasari, Y., Prasetyo, S., Suliyanti, M.M., 2018. The 1064 nm laser-induced breakdown spectroscopy (LIBS) inspection to detect the nutrient elements in freshly cut carrot samples. J. Phys. Conf. Ser 985, 1–6.

Zhang, P., Ma, Y., Liu, S., Wang, G., Zhang, Junzhe, He, X., Zhang, Jing, Rui, Y., Zhang, Z., 2017a.

613 Phytotoxicity , uptake and transformation of nano-CeO 2 in sand cultured romaine lettuce *.
614 Environ. Pollut. 220, 1400–1408. https://doi.org/10.1016/j.envpol.2016.10.094
615 Zhang, P., Ma, Y., Zhang, Z., He, X., Zhang, J., Guo, Z., Tai, R., Zhao, Y., Chai, Z., 2012.
616 Biotransformation of Ceria Nanoparticles in Cucumber Plants. ACS Nano 9943–9950.
617 https://doi.org/10.1021/nn303543n
618 Zhang, P., Xie, C., He, X., Zhang, Z., Ding, Y., Zheng, L., Zhang, J., 2017b. Shape-Dependent
619 Transformation and Translocation of Ceria Nanoparticles in Cucumber Plants. Environ. Sci.
620 Technol. Lett. 4, 380–385. https://doi.org/10.1021/acs.estlett.7b00359
621 Zhang, W., Dan, Y., Shi, H., Ma, X., 2017a. Elucidating the mechanisms for plant uptake and in-
622 planta speciation of cerium in radish (Raphanus sativus L .) treated with cerium oxide
623 nanoparticles. J. Environ. Chem. Eng. 5, 572–577. https://doi.org/10.1016/j.jece.2016.12.036
624 Zhang, W., Ebbs, S.D., Musante, C., White, J.C., Gao, C., Ma, X., 2015. Uptake and Accumulation of
625 Bulk and Nanosized Cerium Oxide Particles and Ionic Cerium by Radish (Raphanus sativus L.).
626 J. Agric. Food Chem. 63, 382–390. https://doi.org/10.1021/jf5052442
627 Zhang, W., Musante, C., White, J.C., Schwab, P., Wang, Q., Ebbs, S.D., Ma, X., 2017b.
628 Bioavailability of cerium oxide nanoparticles to Raphanus sativus L. in two soils. Plant Physiol.
629 Biochem. 110, 185–193. https://doi.org/10.1016/j.plaphy.2015.12.013
630 Zhang, Z., He, X., Zhang, H., Ma, Y., Zhang, P., Ding, Y., Zhao, Y., 2011. Uptake and distribution of
631 ceria nanoparticles in cucumber plants. Metallomics 3, 816–822.
632 https://doi.org/10.1039/c1mt00049g
633 Zhao, L., Peralta-videa, J.R., Rico, C.M., Hernandez-viezcas, J.A., Sun, Y., Niu, G., Servin, A.,
634 Nunez, J.E., Duarte-gardea, M., Gardea-torresdey, J.L., 2014. CeO 2 and ZnO Nanoparticles
635 Change the Nutritional Qualities of Cucumber (Cucumis sativus). J. Agric. Food Chem. 62,
636 2752–2759. https://doi.org/10.1021/jf405476u
637 Zhao, L., Sun, Y., Hernandez-Viezcas, J.A., Servin, A.D., Hong, J., Niu, G., Peralta-Videa, J.R.,
638 Duarte-Gardea, M., Gardea-Torresdey, J.L., 2013. Influence of CeO2 and ZnO nanoparticles on
639 cucumber physiological markers and bioaccumulation of Ce and Zn: A Life Cycle Study. J.
640 Agric. Food Chem. 61, 11945–11951. https://doi.org/10.1021/jf404328e
641

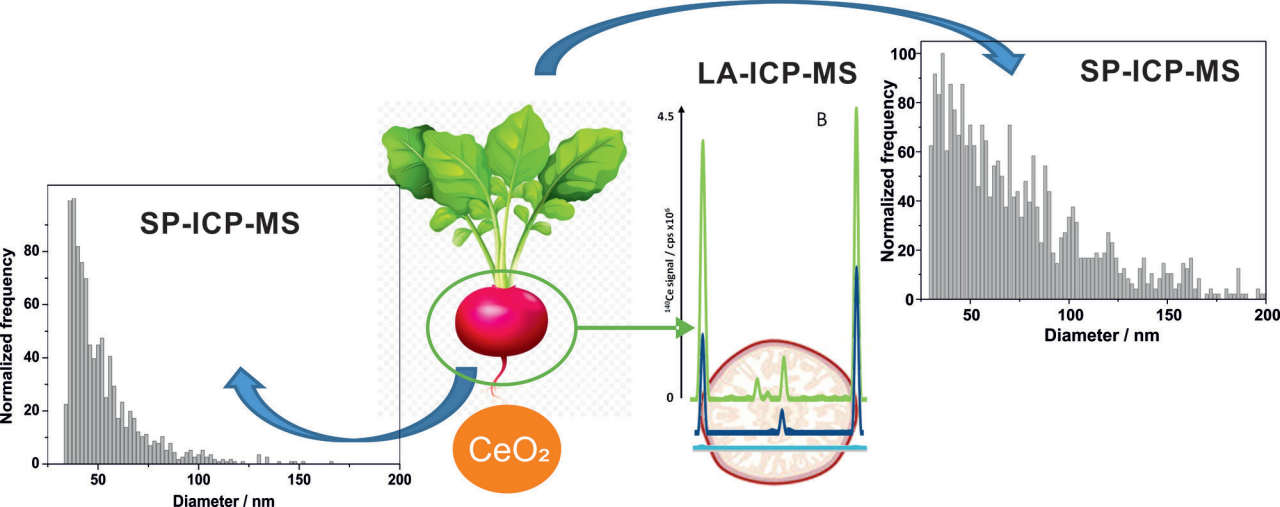
SP-ICP-MS
Normalized frequency
Diameter / nm
CeO2
LA-ICP-MS
B
4.5
0
SP-ICP-MS
Normalized frequency
Diameter / nm